The Monte Carlo Method: Versatility Unbounded In A Dynamic Computing World
Chattanooga, Tennessee, April 17–21, 2005, on CD-ROM, American Nuclear Society, LaGrange Park, IL (2005)

MONTE CARLO METHODS DEVELOPMENT FOR A CONTINUOUS-ENERGY VERSION OF KENO

M. E. Dunn, N. M. Greene, D. F. Hollenbach, and L. M. Petrie
Oak Ridge National Laboratory*
P.O. Box 2008
Oak Ridge, TN 37831-6170, USA
dunnme@ornl.gov; greenenm@ornl.gov; hollenbachdf@ornl.gov; petrielmjr@ornl.gov

ABSTRACT

KENO V.a and KENO VI are Monte Carlo codes that solve the multigroup form of the Boltzmann transport equation and are used for performing criticality calculations of systems with fissionable material. As part of current research at Oak Ridge National Laboratory, continuous-energy or pointwise versions of the KENO codes are being developed for implementation in the SCALE system. Moreover, continuous-energy cross-section processing and transport procedures have been developed to support the Point KENO development. As part of the continuous-energy cross-section development, new procedures based on pointwise collision kinematics have been developed and implemented in the KENO codes. In addition, AMPX cross-section processing modules have been developed for processing ENDF/B evaluations and generating continuous-energy cross-section data for the pointwise versions of KENO. For this work, 50 ENDF/B-VI Release 7 evaluations have been processed to generate a continuous-energy KENO test library. Using the test cross-section library, the continuous-energy transport procedures have been tested by calculating various test problems and comparing with MCNP4C. The details of the continuous-energy transport development and comparison calculations with MCNP are presented in this paper.

Key Words: Monte Carlo, continuous energy, KENO, SCALE

1 INTRODUCTION

For radiation transport applications, completely independent calculational methods are often essential for establishing and verifying safety margins. Work at Oak Ridge National Laboratory (ORNL) has led to the development of cross-section processing and radiation transport methods that are independent of other transport codes used for various radiation transport applications. Both KENO V.a and KENO VI are Monte Carlo (MC) codes that are developed and maintained at the ORNL as part of the SCALE [1] (Standardized Computer Analyses for Licensing Evaluation) system. Historically, the KENO series of codes has been limited to solving the multigroup (MG) form of the Boltzmann transport equation. The objective of this work is to develop and implement in SCALE versions of KENO V.a and KENO VI that utilize continuous-energy or pointwise cross sections to model the radiation transport.

* Managed by UT-Battelle, LLC, under contract DE-AC05-00OR22725 with the U.S. Department of Energy

Continuous-energy versions of KENO V.a and KENO VI have been developed and are currently being tested at ORNL. Hereafter, the term Point KENO will be used to refer to both continuous-energy versions of KENO V.a and KENO VI. Point KENO has been developed by first designing a new continuous-energy cross-section format and secondly by developing the corresponding MC transport procedures to sample the new cross-section format. In addition, multiple cross-section processing modules have been developed for the AMPX-2000 cross-section processing system [2] developed and maintained at ORNL. The essential components of a Point KENO library include (1) the average number of neutrons produced by fission, $\bar{\nu}$ (E); (2) one-dimensional (1-D) continuous-energy cross sections as a function of temperature, σ (E, T); (3) two-dimensional pointwise joint probability distributions that describe the energy and angle of particles emerging from a collision, f(E→E′, μ); and (4) probability tables for sampling the cross sections in the unresolved-resonance region. An overview of the cross-section processing methods and radiation transport procedures for Point KENO has been published previously [3, 4]. Furthermore, details concerning the AMPX procedures for generating probability tables for Point KENO in the unresolved-resonance region have also been published previously [5]. The objective of this paper is to present the collision kinematics modeling theory for use in Point KENO.

2 COLLISION KINEMATICS THEORY

In the MC simulation of particle interactions, the energy and angle of the exiting particle are needed to simulate the radiation transport. During a collision, the kinematics of the exiting particle can be specified by more than one random variable. If the two random variables are not stochastically independent in the case of exit energy and angle, a coupled or joint doubly differential probability function must be defined to represent the collision kinematics. The ENDF data [6] can provide either a coupled or independent energy-angle representation. In particular, ENDF/B Files 4 and 5 can be used to present the singly differential probability density function (PDF) for the angular and energy distribution of secondary neutrons, respectively. The data presented in Files 4 and 5 are independent PDFs. With the release of ENDF/B-VI, the File 6 formats can be used to specify coupled PDFs for the energy-angle distribution of secondary neutrons. Because the independent PDF representation can be considered as a subset of the coupled representation, the following discussion is devoted to processing the coupled energy-angle PDF.

The data in ENDF/B File 6 provide the joint PDF $f(E', \mu)$ for producing an exit energy and angle due to a collision with the target isotope/nuclide at an incident energy E. The joint PDF is a normalized distribution such that the following condition is valid:

$$\int dE' \int d\mu \, f(E', \mu) = 1. \tag{1}$$

For the purposes of discussion, let the variable $x = E'$ and the variable $y = \mu$. Therefore, the corresponding joint cumulative distribution function (CDF) can be defined as follows:

$$F(x, y) = P(\xi \le x, \eta \le y). \tag{2}$$

The joint CDF defines the probability that the random variables ξ and η are less than or equal to x and y, respectively. In addition, the PDF is related to the CDF as follows:

$$f(x,y) = \frac{d^2F(x,y)}{dx\,dy} = \frac{d^2F(x,y)}{dy\,dx}. \tag{3}$$

For stochastically independent variables, the CDF can be separated as follows:

$$F(x,y) = G(x)\,H(y). \tag{4}$$

Equation (4) implies that the CDF can be decoupled into two separate distributions G and H; however, if the two variables are coupled, Eq. (4) is no longer valid:

$$F(x,y) \neq G(x)\,H(y). \tag{5}$$

The CDFs for thermal scattering and ENDF/B-VI File 6 representations are coupled distributions and Eq. (4) is not valid for these distributions.

For the purposes of discussion, a "marginal" CDF can be defined for the variable x, $F(x, \infty)$. The marginal CDF represents the probability that $\xi \leq x$ while permitting η to vary freely. In other words, the value for η has not been selected. The corresponding marginal PDF for x is defined as follows:

$$f(x,\infty) = \int_{-\infty}^{\infty} f(x,y)\,dy = \frac{dF(x,\infty)}{dx}. \tag{6}$$

Based on Eq. (6), the marginal PDF for x is obtained by integrating the joint PDF over all phase space of the variable y. The selection of x must be sampled from the marginal CDF, which is obtained by integrating the marginal PDF with respect to x:

$$F(x,\infty) = \int_{-\infty}^{x} f(\xi,\infty)\,d\xi\ . \tag{7}$$

The resulting expression in Eq. (7) is set equal to a random number (R_1), and the resulting equation is solved for x. In the subsequent discussion, the sampled value of x will be denoted as $\hat{x}$,which is a scalar quantity. Once the value of $\hat{x}$ is obtained, the normalization condition is imposed:

$$\int_{-\infty}^{\infty} \left[\frac{f(\hat{x},y)}{f(\hat{x},\infty)}\right] dy = 1. \tag{8}$$

Once the selection for $\hat{x}$ is made, the PDF for the remaining unspecified variable y is denoted as $g(y \mid \hat{x})$ and is referred to as the conditional PDF for y. In other words, the quantity $\hat{x}$ has been sampled, and the resulting PDF for y is conditional upon the sampled value for the variable x. Therefore, Eq. (8) represents the normalization condition for the conditional PDF for y. The conditional PDF for y is expressed as follows:

$$g(y \mid \hat{x}) = \frac{f(\hat{x}, y)}{f(\hat{x}, \infty)}. \tag{9}$$

The conditional CDF for y is obtained by integrating $g(y \mid \hat{x})$ with respect to y:

$$G(y \mid \hat{x}) = \int_{-\infty}^{y} g(\eta \mid \hat{x})\, d\eta = \int_{-\infty}^{y} \left[\frac{f(\hat{x}, \eta)}{f(\hat{x}, \infty)} \right] d\eta = \frac{F(\hat{x}, y)}{f(\hat{x}, \infty)}. \tag{10}$$

In order to select the value for y, the resulting expression from Eq. (10) is set equal to a random number (R_2) and the equation is solved for y. The sampled value for y is denoted $\hat{y}$.

In the preceding discussion, the MC sampling procedure starts with the x variable (i.e., marginal on x) and concludes with sampling the y variable (conditional on y). The process could also be performed with the marginal operation on the y variable and the conditional operation on the x variable. Therefore, the order of selection is somewhat arbitrary; however, the ease of selecting one variable prior to the other variable may dictate the selection order. For the Point KENO development, the decision was made to formulate the probability distributions for the collision kinematics with the marginal selection operation applied to the exit angle cosine, μ, and the conditional selection operation applied to the exit energy variable, E. Additional details concerning the Point KENO collision sampling procedures are provided in the following section.

3 KINEMATICS SAMPLING

One of the novel and robust features of the latest AMPX cross-section processing system is the new treatment of the collision kinematics data that provide secondary energy and angle distributions for particles emerging from a reaction of interest. In AMPX, a "universal" tabular kinematics structure (i.e., data have the same structure independent of reaction type) has been developed to describe all possible secondary energy-angle distributions including thermal scattering collisions. Because the most complicated kinematics structure is for coupled energy-angle distributions, the AMPX collision kinematics format is formulated to address the coupled distributions, with all other collision formats being a subset of the coupled distribution. As a result, the independent kinematics distributions (i.e., no coupling between energy and angle) can be organized and stored in the same format as the coupled distributions. Note that this approach does not "magically" create coupled distributions from stochastically independent distributions; rather, the approach is to store the tabular kinematics data in a uniform fashion such that the subsequent processing and transport procedures do not need to determine whether there is a coupling between energy and angle. Because of the uniformity in the collision kinematics data, pointwise cross-section libraries can be produced that are independent of ENDF laws and

procedures. Some continuous-energy radiation transport codes have the ENDF laws and procedures programmed in the transport code. Unfortunately, as changes are made to the ENDF formats, the radiation transport code and associated cross-section processing code system must be updated to process the new ENDF laws and procedures. Because of the novel AMPX processing procedures, the burden of treating ENDF formats in the transport code has been placed solely on the cross-section processing system.

AMPX is used to process the ENDF/B collision kinematics data and generate probability distributions for particle exiting energies and angles in the lab system frame of reference. The AMPX kinematics distributions have the general structure as shown in Table I where the angular representation is provided in the form of Legendre moments of the angular distribution with special procedures to treat singular coupled distributions such as for elastic scatter and discrete-level inelastic scatter. Note that a standard Legendre expansion cannot be used to represent the discrete processes because an infinite number of terms would be required to represent the Dirac delta function.

Table I. General structure of AMPX kinematics data

Energy Transfer	**ℓ = 0**	**ℓ = 1**		**ℓ = NL**
$\mathbf{E_1 \rightarrow E'_1}$	$M_0(E_1 \rightarrow E'_1)$	$M_1(E_1 \rightarrow E'_1)$	·····	$M_{NL}(E_1 \rightarrow E'_1)$
$\mathbf{E_1 \rightarrow E'_2}$	$M_0(E_1 \rightarrow E'_2)$	$M_1(E_1 \rightarrow E'_2)$	·····	$M_{NL}(E_1 \rightarrow E'_2)$
⋮	⋮	⋮		⋮
$\mathbf{E_1 \rightarrow E'_{NF}}$	$M_0(E_1 \rightarrow E'_{NF})$	$M_1(E_1 \rightarrow E'_{NF})$	·····	$M_{NL}(E_1 \rightarrow E'_{NF})$
$\mathbf{E_{NE} \rightarrow E'_1}$	$M_0(E_{NE} \rightarrow E'_1)$	$M_1(E_{NE} \rightarrow E'_1)$	·····	$M_{NL}(E_{NE} \rightarrow E'_1)$
$\mathbf{E_{NE} \rightarrow E'_2}$	$M_0(E_{NE} \rightarrow E'_2)$	$M_1(E_{NE} \rightarrow E'_2)$	·····	$M_{NL}(E_{NE} \rightarrow E'_2)$
⋮	⋮	⋮		⋮
$\mathbf{E_{NE} \rightarrow E'_{NF}}$	$M_0(E_{NE} \rightarrow E'_{NF})$	$M_1(E_{NE} \rightarrow E'_{NF})$	·····	$M_{NL}(E_{NE} \rightarrow E'_{NF})$

$M_\ell(E \rightarrow E')$: angular moment for transfer from $E \rightarrow E'$
ℓ: order of the angular moment
NL: maximum order of the Legendre expansion
NE: total number of incident energies
NF: total number of exit energies

In terms of Legendre polynomials, the joint collision kinematics PDF has the form

$$f(E \rightarrow E', \mu) = \sum_{\ell=0}^{\infty} \frac{2\ell+1}{2} f_\ell P_\ell(\mu) \tag{11}$$

where

$$f_\ell(E \rightarrow E') = \sum_{i=0}^{\ell} p_{\ell i} \int_{-1}^{1} f(E \rightarrow E', \mu) \mu^i \, d\mu = \sum_{i=0}^{\ell} p_{\ell i} M_i(E \rightarrow E'). \tag{12}$$

In Eq. (12), $p_{\ell i}$ represents the coefficients of the Legendre polynomial. AMPX provides the angular moments of the distribution, $M_\ell(E \rightarrow E')$, as a function of incident energy for each kinematics reaction provided in the ENDF/B evaluation. Substituting the expression for f_ℓ into Eq. (11) provides the following expression for the joint PDF:

$$f(E \rightarrow E', \mu) = \sum_{\ell=0}^{NL} \frac{2\ell+1}{2} P_\ell(\mu) \sum_{i=0}^{\ell} p_{\ell i} M_i(E \rightarrow E'). \tag{13}$$

In Eq. (13), the distribution is truncated at a maximum order of expansion NL. Typically, a 5th order expansion is sufficient to calculate the moments of the kinematics distributions.

As noted previously, the exit angle cosine, μ, is selected first in the Point KENO collision kinematics process. By integrating Eq. (13) over all exit energies, the corresponding marginal PDF for Point KENO is defined as follows:

$$f(\infty, \mu) = \int_{E'_{min}}^{E'_{NF}} f(E \rightarrow E', \mu) dE' = \sum_{\ell=0}^{NL} \frac{2\ell+1}{2} P_\ell(\mu) \sum_{i=0}^{\ell} p_{\ell i} \int_{E'_{min}}^{E'_{NF}} M_i(E \rightarrow E') dE'. \tag{14}$$

In Eq. (14), E'_{min} is the minimum possible exit energy for the reaction, and E'_{NF} is the maximum possible exit energy for the reaction. By defining I_i as the integral of the angular moments over all exit energies, the marginal PDF for selecting the exit angle cosine becomes

$$f(\infty, \mu) = \sum_{\ell=0}^{NL} \frac{2\ell+1}{2} P_\ell(\mu) \sum_{i=0}^{\ell} p_{\ell i} I_i . \tag{15}$$

To select the exit cosine, the marginal PDF in Eq. (15) must be converted to the marginal CDF by integrating over the possible exit cosines:

$$F(\infty, \mu) = \int_{-1}^{\mu} f(\infty, y') dy' = \sum_{\ell=0}^{NL} \frac{2\ell+1}{2} \sum_{i=0}^{\ell} p_{\ell i} I_i \int_{-1}^{\mu} P_\ell(y') dy' . \tag{16}$$

For anisotropic distributions, the above marginal CDF is used to construct tabular distributions for selecting the exiting angle cosine as a function of incident energy. If the angular distribution is isotropic, the exit angle cosine is sampled uniformly from -1 to 1.

Once the exit angle cosine, $\hat{\mu}$, is selected, the exit energy must be sampled, and the conditional PDF for selecting the exit energy is defined as follows:

$$g(E' \mid \hat{\mu}) = \frac{f(E', \hat{\mu})}{f(\infty, \hat{\mu})}. \tag{17}$$

In Eq. (17), $f(\infty, \hat{\mu})$ is the normalization condition for the conditional PDF and is obtained by evaluating Eq. (15) at the selected exit angle cosine. The conditional CDF for selecting the exit energy is obtained by integrating Eq. (17) over the possible exit energies:

$$G(E' \mid \hat{\mu}) = \int_{E'_{min}}^{E'} \frac{f(x', \hat{\mu})}{f(\infty, \hat{\mu})} dx' = \frac{1}{f(\infty, \hat{\mu})} \sum_{\ell=0}^{NL} \frac{2\ell+1}{2} P_\ell(\hat{\mu}) \sum_{i=0}^{\ell} p_{\ell i} \int_{E'_{min}}^{E'} M_i(E \to x') dx'. \tag{18}$$

The conditional CDF $G(E' \mid \hat{\mu})$ is used to construct tabular distributions for Point KENO in order to select the exiting energy as a function of incident energy and exiting angle cosine.

The kinematics data in the Point KENO library are provided in the lab or target-at-rest system as opposed to the center-of-mass system (COM). By adhering to the lab coordinate system, Point KENO does not have to transform between different coordinate systems during the random walk; however, the energy and angle representations for certain reactions (elastic scattering, discrete-level inelastic scattering, etc.) become more complex in the lab system. For example, an angular distribution that is isotropic in the COM is anisotropic in the lab system. Moreover, the secondary distribution as a function of exit angle in the lab system can be "double-valued" (i.e., two exit energies for the same angle cosine) for certain reaction incident energies (i.e., hydrogen elastic scattering and discrete-level inelastic scattering). Consequently, special care is exercised in the construction of secondary angle and energy distributions for Point KENO.

For each reaction in the Point KENO kinematics structure, exit angle cosine distributions are tabulated as a function of incident energy. The kinematics format permits the anisotropic distributions to be expressed in either equiprobable or non-equiprobable cosine bins. Moreover, the kinematics format permits the number of secondary angles to vary as a function of incident energy. For each incident energy-angle cosine pair [i.e., (E, μ)], there is a corresponding exit energy distribution. As with the angular data, the secondary energy distributions may be provided in either equiprobable or non-equiprobable energy bins. The number of secondary energies can vary as a function of each (E, μ) pair.

The Point KENO kinematics format is designed to accommodate coupled angle-energy distributions of secondary particles. Moreover, interpolation procedures are used to obtain intermediate angle or energy values between tabulated angle or energy values. As noted previously, special cases can be accommodated as a subset of the Point KENO kinematics format. For isotropic angular distributions, the kinematics data specify a single exit cosine with a nonphysical value of -2 as a function of incident energy, thereby signaling an isotropic distribution. As a result, the exit angle cosine is sampled uniformly between -1 and 1. Because the exit energy distribution is stochastically independent of the angle distribution, the exit energy distribution reduces to being only a function of incident energy.

For elastic and discrete-level inelastic scattering, the doubly differential distribution contains a Dirac delta function because there is a one-to-one correspondence between the exiting angle and energy. Once the exiting angle is selected, the exiting energy is fixed by virtue of the kinematics equations that are documented in most conventional reactor theory textbooks. Angular cosine distributions are constructed as a function of incident energy, and the exit angle cosine is sampled depending on the type of distribution (i.e., isotropic or anisotropic). Except for the double-value region in the lab system, there is one possible exiting energy value for each (E, μ) during elastic and discrete-level inelastic scattering collisions. Therefore, the exit energy distribution in the kinematics data has a single secondary energy with a probability of 1 corresponding to each (E, μ). For the double-value region, there are two possible exit energies for each (E, μ), and the exit energy distribution has two secondary energies with different probabilities corresponding to each (E, μ).

With regard to thermal scattering data, coherent and incoherent elastic scattering results in no energy change following a collision. As a result, the kinematics data have exit angle distributions tabulated as a function of incident energy, and the corresponding secondary energy distribution block for each (E, μ) has a single exit energy value equal to the incident energy. For incoherent inelastic scattering data [i.e., $S(\alpha,\beta)$], the angle-energy distributions are coupled and easily accommodated in the Point KENO kinematics format. If thermal scattering data are not provided in the ENDF/B evaluation, elastic scattering kinematics data are constructed using the free-gas approximation.

4 RESULTS

For the Point KENO development, AMPX modules were developed to post-process the pointwise collision kinematics data provided by AMPX modules that existed prior to the Point KENO development. The new AMPX processing modules have been used to generate continuous-energy cross-section data for 50 ENDF/B-VI Release 7 nuclides that include collision kinematics data as described in the previous sections. The test library includes all the uranium and plutonium isotopes, in addition to thermal data for H in H_2O and H in CH_2. Various critical benchmark experiments have been calculated using Point KENO V.a, and comparisons have been made with MCNP4C [7] for verification purposes. The Point KENO–calculated results for the criticality problems are in agreement with calculated results obtained with the multigroup version of KENO V.a and MCNP4C. The results of the Point KENO criticality benchmark calculations are presented in References [3] and [4] and are not repeated in this paper.

In order to demonstrate the computational capabilities that have been developed for the collision kinematics data, a MC code (SPARTICUS—**S**lab **P**ointwise **A**djoint **R**esearch **T**ool **I**n **C**lever **U**sable **S**oftware) was developed to test the Point KENO cross-section data to perform a forward or adjoint continuous-energy neutron transport calculation through a user-defined slab of material. Because KENO can be used only for criticality calculations, SPARTICUS was developed to perform 1-D fixed source calculations through a slab in order to test the same continuous-energy transport procedures that are used in Point KENO. Also, SPARTICUS has been developed to demonstrate a pointwise-energy adjoint transport capability; however, additional research must be completed before the adjoint capability is completely functional. In order to test the collision kinematics procedures, SPARTICUS was used to perform forward transport calculations through slabs of potassium and hydrogen with varying thicknesses. For each case, the slab of material was exposed to a monoenergetic and monodirectional neutron source incident on the x = 0 cm face. Various source strengths were used in the computational studies, and flux and particle tallies were computed at the incident and exit faces of each slab. Comparison calculations were also performed with MCNP4C using cross sections that are based on the same ENDF/B-VI Release 7 evaluations used by Point KENO and SPARTICUS; however, the MCNP cross-section data were prepared using the NJOY [8] code system. All of the MC calculations were performed with 3 million histories.

Potassium has 17 discrete-level inelastic reactions, and there is a double-value region for each discrete-level inelastic reaction in the lab system. The size (i.e., in terms of energy range above the inelastic threshold) of the double-value region is a function of the reaction Q value and the mass of the target nuclide. For potassium, the size of the double value region for the discrete-level inelastic reactions ranges between 1.73 and 4.4 keV. In contrast, hydrogen has a double-value region that spans the entire incident energy range for elastic scattering in the lab system. As a result, hydrogen and potassium were selected to test the pointwise collision kinematics procedures because of the additional complexity involved with modeling the double-value region kinematics. Note that MCNP models the elastic scattering and discrete-level inelastic scattering in the COM using analytic kinematics equations. In contrast, the Point KENO and SPARTICUS collision kinematics are modeled in the lab system using tabulated kinematics data. The use of uniform tabular kinematics distributions has been implemented in preparation for the development of the continuous-energy adjoint transport capability. Therefore, the MCNP calculations provide an independent method for verifying the collision kinematics procedures of this work.

Figures 1 and 2 provide the particle leakage results from SPARTICUS and MCNP at the x = 0 cm and x = 100 cm faces, respectively, of a 100-cm-thick potassium slab exposed to a 1.5-MeV neutron source. For the hydrogen case, a 100-cm-thick slab is exposed to a 100 keV neutron source, and the particle leakage is plotted at the x = 0 cm face and the 100 cm face in Figs. 3 and 4, respectively. The magnitude of the standard deviation on the particle tallies is too small to see in the plots and is not included in the figures. For the potassium transmission calculations, the standard deviations for the particle tally results from both MCNP and SPARTICUS agree and range between 10^{-3} and 10^{-6}. Likewise, the standard deviations for the MCNP and SPARTICUS

hydrogen transmission calculations agree and range between 10^{-4} and 10^{-6}. As shown in Figs. 1 through 4, the SPARTICUS particle tallies agree with the MCNP results. Moreover, both sets of transmission calculations exhibit a backscatter component that is shown in both the MCNP and SPARTICUS results for hydrogen and potassium at the x = 0 cm surface. Furthermore, particle leakage at the exit surface (x = 100 cm) of each slab agrees for both MC transport calculations.

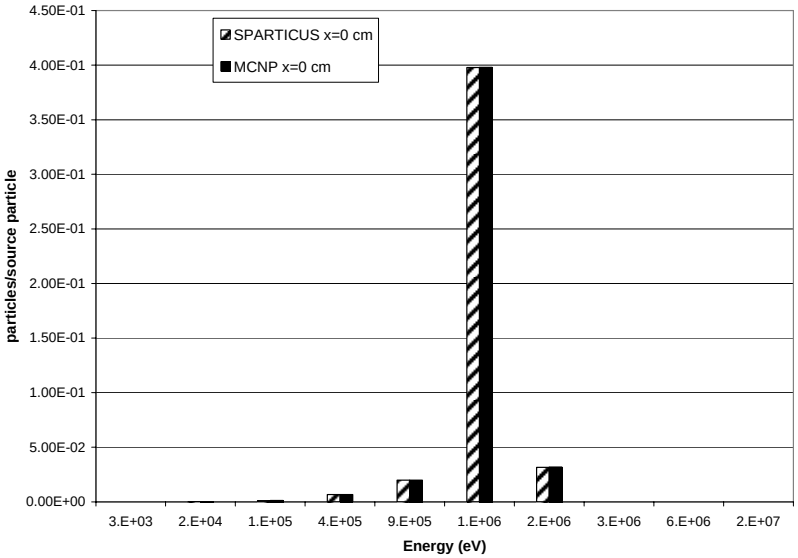

Figure 1. Particle leakage comparison between SPARTICUS and MCNP4C at the x = 0 cm face of a 100-cm-thick potassium slab exposed to a 1.5-MeV monoenergetic and monodirectional neutron source at x = 0 cm.

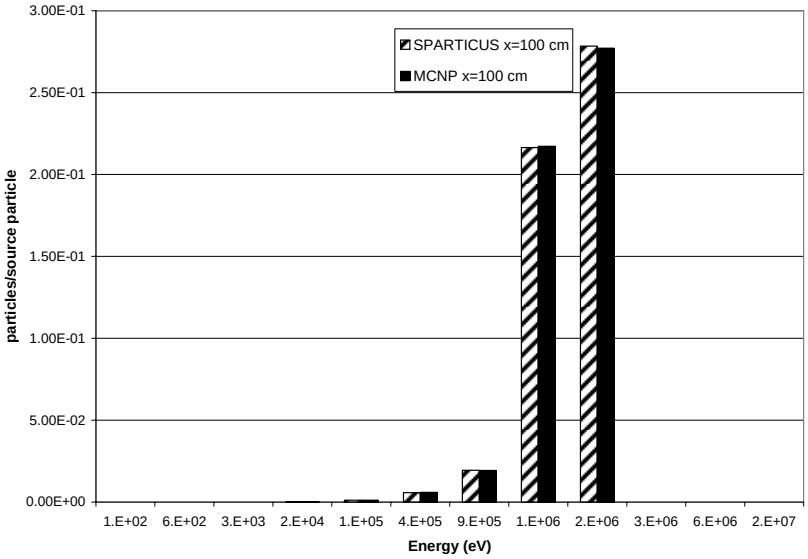

Figure 2. Particle leakage comparison between SPARTICUS and MCNP4C at the x = 100 cm face of a 100-cm-thick potassium slab exposed to a 1.5-MeV monoenergetic and monodirectional neutron source at x = 0 cm.

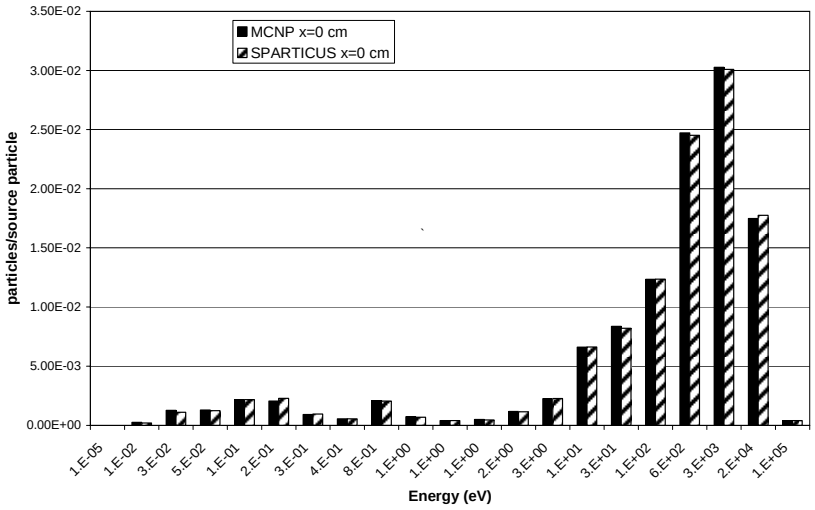

Figure 3. Particle leakage comparison between SPARTICUS and MCNP4C at the x = 0 cm face of a 100-cm-thick hydrogen slab exposed to a 100-keV monoenergetic and monodirectional neutron source at x = 0 cm.

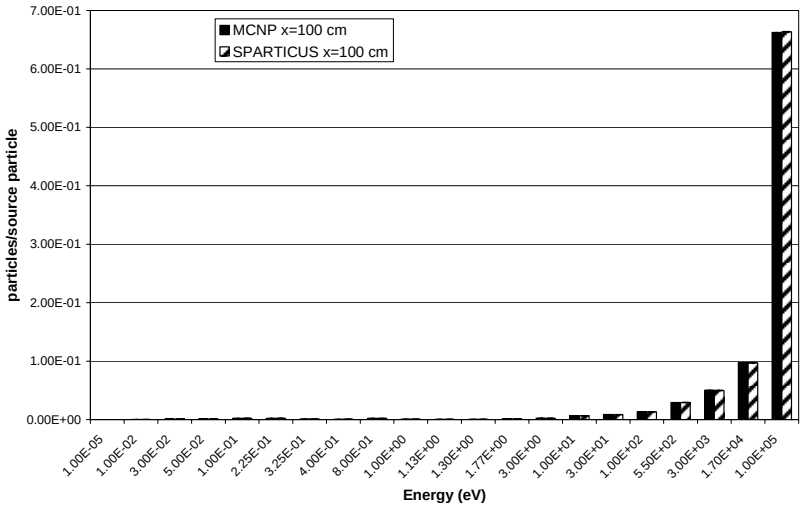

Figure 4. Particle leakage comparison between SPARTICUS and MCNP4C at the x = 100 cm face of a 100-cm-thick hydrogen slab exposed to a 100-keV monoenergetic and monodirectional neutron source at x = 0 cm.

5 SUMMARY

The objective of the research is to develop and demonstrate MC collision kinematics procedures that are used in continuous-energy versions of the ORNL MC codes KENO V.a and KENO VI. The initial phase of the research focused on the design and development of a continuous-energy cross-section format and the associated cross-section processing modules for the AMPX code system. A new approach to treat continuous-energy collision kinematics procedures has been developed as part of the cross-section development phase of the research. After defining the cross-section format, transport procedures were developed and implemented in continuous-energy versions of KENO V.a and KENO VI. Subsequently, 50 ENDF/B-VI Release 7 nuclides were processed with AMPX to create a test pointwise cross-section library. The continuous-energy transport procedures have been tested by calculating various criticality and computational test problems. In addition, a prototypic 1-D fixed source MC transport code SPARTICUS has been developed to further test the continuous-energy collision kinematics procedures and compare with MCNP4C calculations. SPARTICUS and Point KENO use the same continuous-energy cross-section data and have the same transport procedures. The continuous-energy collision transport procedures have been demonstrated by performing fixed source transmission calculations through slabs of hydrogen and potassium that are exposed to monoenergetic and monodirectional neutron sources. The particle leakage results from the transmission calculations agree with results obtained with MCNP4C and successfully demonstrate the continuous-energy Point KENO collision kinematics procedures.

6 ACKNOWLEDGMENTS

The Point KENO development was sponsored by the United States Nuclear Regulatory Commission. The development of the continuous-energy transport code SPARTICUS was completed under the ORNL Laboratory Directed Research and Development (LDRD) Seed Money Program.

7 REFERENCES

1. "SCALE: A Modular Code System for Performing Standardized Computer Analysis for Licensing Evaluation," NUREG/CR-0200, Rev. 7 (ORNL/NUREG/CR/CSD-2/R7), Vols. I, II, and III, May 2004 (Draft). Available from Radiation Safety Information Computational Center at Oak Ridge National Laboratory as CCC-725.
2. M. E. Dunn and N. M. Greene, "AMPX-2000: A Cross-Section Processing System for Generating Nuclear Data for Criticality Safety Applications," *Trans. Am. Nucl. Soc.,* **86**, pp. 118-119 (2002).
3. M. E. Dunn, N. M. Greene, and L. M. Petrie, "Continuous-energy Version of KENO V.a for Criticality Safety Applications," *Proceedings of the 7th International Conference on Nuclear Criticality Safety, ICNC 2003*, Tokai, Ibaraki, Japan, Oct. 20-24, 2003.
4. M. E. Dunn, N. M. Greene, and L. M. Petrie, "Point KENO V.a: Continuous-energy Monte Carlo Code for Transport Applications," *Proceedings of PHYSOR 2004: The Physics of Fuel Cycles and Advanced Nuclear Systems: Global Developments*, Chicago, Ill., April 25-29, 2004.

5. M. E. Dunn and L. C. Leal, "Calculating Probability Tables for the Unresolved-Resonance Region Using Monte Carlo Methods," *Nucl. Sci. & Eng.*, **148**, pp. 1-13 (2004).
6. "ENDF-102 Data Formats and Procedures for the Evaluated Nuclear Data File ENDF-6," BNL-NCS-44945-01/04-Rev., Brookhaven National Laboratory, April 2001.
7. "MCNP—A General Monte Carlo – Particle Transport Code," Version 4C, LA-13709-M, J. F. Briesmeister, Ed., Los Alamos National Laboratory, (2000).
8. R. E. MacFarlane and D. W. Muir, "NJOY99.0 Code System for Producing Pointwise and Multigroup Neutron and Photon Cross Sections from ENDF/B Data," PSR-480/NJOY99.0, Los Alamos National Laboratory, March 2000.